Sediments within the icy North Polar Deposits of Mars record recent Impacts and Volcanism

Prakhar Sinha[1] and Briony Horgan[1]

[1]Department of Earth, Atmospheric, and Planetary Sciences, Purdue University.

Corresponding author: Prakhar Sinha (sinha37@purdue.edu)

Key Points:

- CRISM spectra show crystalline and glass-rich mafic sediments are present throughout the north polar layered deposits
- Composition, grainsize, and heterogeneity of sediments suggest impact and volcanic sources
- These non-dust lithics within the north polar deposits are suitable for in-situ dating of ice cores and constraining climate models

Abstract

The North Polar Layered Deposits (NPLD) of Mars are ice-rich sedimentary layers that formed under the influence of Mars' modern climate and thus record the recent climatic history of Mars, analogous to terrestrial ice sheets. The 2013-2023 Planetary Science Decadal Survey recommends a lander mission to sample the NPLD for climatic records; however, linking the geologic record to the climatic history will require quantitative dating of the NPLD. In this study we use orbital reflectance spectroscopy to show for the first time that dateable mafic lithics are present throughout the NPLD. We find significant glass as well as diverse crystalline minerals, which suggests that surface processes like impacts and volcanism were active during the late Amazonian and transported sediments from across the planet to the north pole. In situ investigation of the NPLD will thus provide critical quantitative constraints on both the recent geologic and climatic histories of Mars.

Plain Language Summary

Mars' north polar cap accumulated over last few millions of years due to seasonal buildup of frost trapping atmospheric gases and incoming sediments, thereby preserving the history of Mars' recent climate in the form of an ice-rich geologic record. Characterizing the contents of these deposits is essential to understand the role of geologic and climatic processes recently active on Mars. The Mars scientific community recommends robotic exploration of these icy north polar deposits to sample the ice and extract climate records. This study uses a novel technique to determine the composition of sediments entrained in ice by analyzing the properties of reflected light from the icy surface which is captured using an imaging spectrometer from orbit. A diverse suite of iron-bearing minerals are detected within sediments eroding from the icy deposits, which we hypothesized were sourced from recent impacts and volcanic eruptions that deposited sediments over the north polar region. Therefore, processes like impacts and volcanism influenced the formation of the north polar deposits. Because the sediments from these sources are dateable, they can be used to determine the age of its ice-rich climate records and thus the timescales of climate change on another planet.

1 Introduction

The polar caps of Mars are the only known modern climate record preserved beyond Earth (Smith et al., 2020). At the north pole, the icy North Polar Layered Deposits (NPLD; **Figure 1**) cap the massive polar plateau, Planum Boreum (Tanaka et al., 2008). The NPLD formed during the late Amazonian period, perhaps as recently as 5 Mya, when variations in the obliquity of Mars caused differences in insolation, leading to periodic accumulation and ablation of volatiles and dust on the poles (Cutts, 1973; Levrard et al., 2007; Schultz & Lutz, 1988; Toon et al., 1980). These deposits are over 3 km thick and contain thousands of layers, each containing a record of surface processes and atmospheric state at the time of deposition (Becerra et al., 2017; Fishbaugh et al., 2010; Smith et al., 2016). *In situ* exploration of these deposits for climate records is a crucial next step towards advancing the field of planetary climatology (Smith et al., 2020). Quantitatively linking this NPLD geologic record to the climatic history will require firm age constraints on its ice-rich sedimentary layers, however, it is unknown if materials suitable for quantitative geochronology exist within the NPLD.

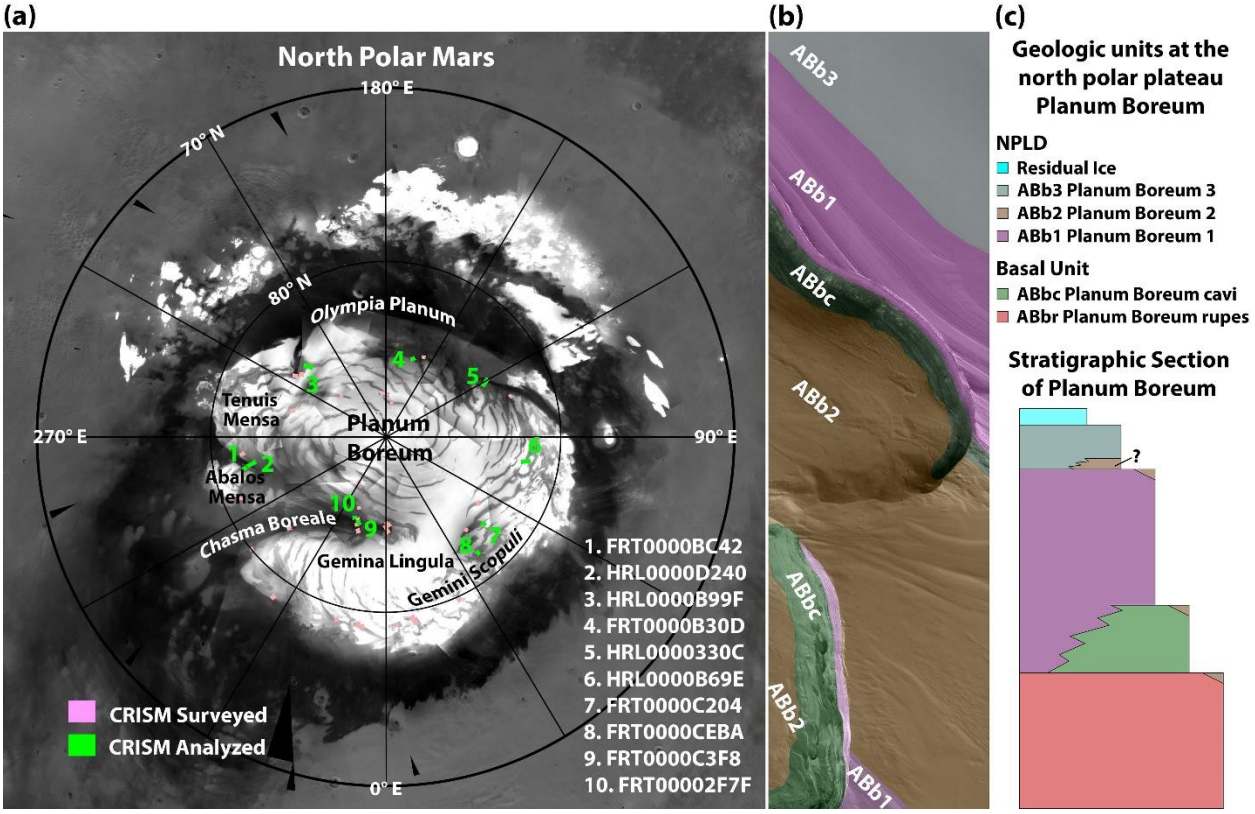

Figure 1: (*a*) Locations of studied CRISM images of NPLD exposures over Mars Orbiter Camera albedo map (NASA/MSSS) showing bright north polar ice cap surrounded by the dark sand sea. (*b*) HiRISE image showing color-coded geologic units at Boreum Cavus in Chasma Boreale. (*c*) General stratigraphy of the north polar plateau, Planum Boreum.

In terrestrial ice core studies, younger ice cores are dated by counting annual layers and dating trapped gasses. But as ice gets older, it loses its annual layers and trapped gases are lost due to subsequent melting, compaction, and diffusion, which increase the uncertainty in the measured ages (Buizert et al., 2014). Therefore, radiometric dating and/or exposure dating of dateable lithic sediment, such as volcanic ash from volcanic eruptions or impact ejecta layers (Basile et al., 2001), entrained in the icy layers is used to constrain the absolute age of the layers. But lithics within the NPLD have previously been assumed to be composed of globally homogenized airfall dust, which is of unknown origin and age. While some models suggest that other more easily datable sediments may exist within the NPLD (Bouška & Bell III, 1993; Kerber et al., 2012), orbital investigations of the composition of the NPLD have focused on hydrated minerals (Horgan et al., 2009; Massé et al., 2010, 2012) and ice grain size (Calvin et al., 2009), so it is unknown whether or not the NPLD contain primary mafic silicates that could indicate dateable volcanic or impact deposits. This study utilizes CRISM high resolution orbital visible/near-infrared hyperspectral images of exposed strata at peripheral scarps and interior troughs in the NPLD, to constrain for the first time the composition, origin, and distribution of dark non-ice materials in the NPLD and to test whether or not the NPLD contain suitable materials for quantitative geochronology.

2 Spectral Diversity in the NPLD

For details of spectral analysis (**Tables S3** and **S4:** spectral data), see methods section in supplementary information, and see **Figure 1a** and **Table S1** for location of CRISM sites. **Figures 2, S2,** and **S3** show CRISM images and their RGB color-composite maps generated using standard CRISM spectral parameters (Viviano-Beck et al., 2014) as listed in **Table S2**.

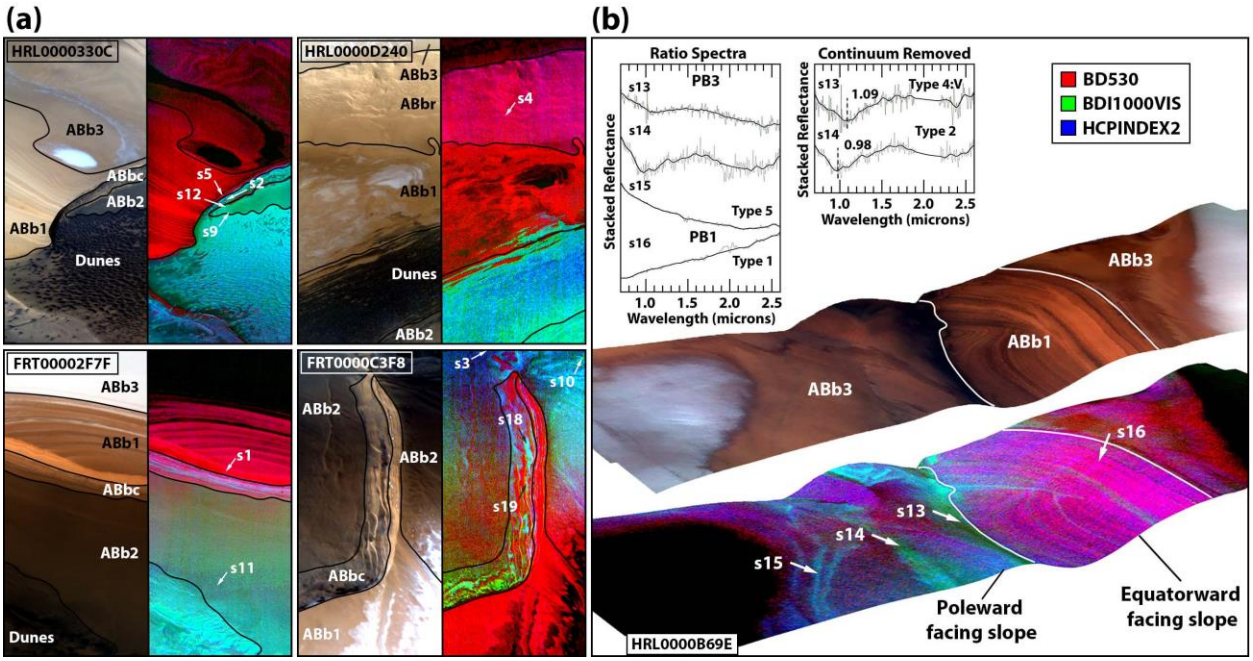

Figure 2: (*a*) CRISM approximate natural color images (See **Figure 1a** for location; **Figures 3** and **4** for labeled spectra), labeled with NPLD stratigraphic units, are paired with RGB color-composites of CRISM summary products BD530 (red), BDI1000VIS (green), and HCPINDEX2 (blue). The spectral parameters measure absorptions at 0.53, 1, and 2 μm which here are indicative of ferric-dust, glass, and HCP, respectively. (*b*) When projected over MOLA elevation model, HRL0000B69E shows a trough whose equatorward facing slope is dust-dominated whereas the poleward facing slope displays strong mafic signatures.

CRISM spectra of NPLD outcrops exhibit signatures due to both water ice and lithic materials, including airfall dust and mafic minerals. NPLD lithics fall into 4 distinct spectral classes (**Figure 3**). After ratioing to bright icy and dusty regions in the same scene (**Figure S4:** spectral processing approach), spectra from regions dominated by nanophase ferric iron oxide in martian dust (Type 1) are spectrally featureless and exhibit strong red spectral slopes (Morris et al., 1997). In contrast, ratio spectra of most dark-toned sediments show broad absorption bands at both 1 and 2 μm, indicative of the presence of iron in mafic minerals. Spectra with broad absorption bands centered between 0.95-1.05 μm and near 2.1 μm are consistent with high-Ca pyroxene (HCP; Type 2; Cloutis & Gaffey, 1991; Horgan et al., 2014), and are similar to regions within the Olympia Undae portion of the circumpolar dune field (Horgan & Bell, 2012). Spectra

with a more symmetric band centered beyond 1.08 μm and a second band near 2.1 μm are consistent with iron-bearing (e.g., basaltic) glass, possibly mixed with some HCP (Type 3; Horgan & Bell, 2012).

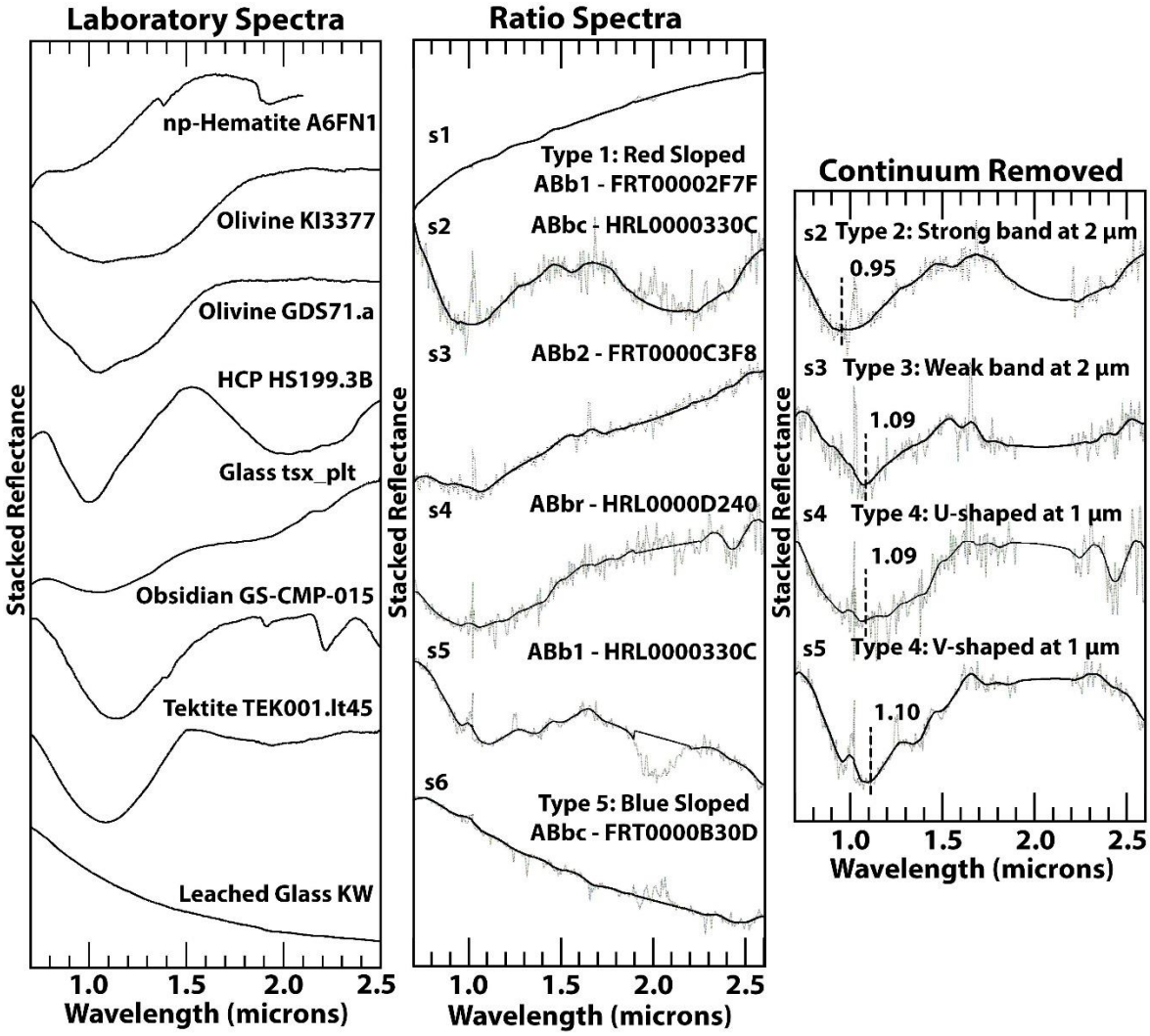

Figure 3: (*Left*) Lab spectra of Fe-bearing minerals (Cloutis & Gaffey, 1991; King & Ridley, 1987; Minitti et al., 2002; Morris & Lauer Jr, 1990). (*Middle*) CRISM ratio spectra of lithic sediments in the NPLD. (*Right*) CRISM continuum removed spectra clearly showing mafic absorption bands. Thick black spectra have been smoothed from underlying thin gray lines. See Figures 2 and S3 for spectra locations.

Other dark sediments exhibit a broad 1 μm absorption band but show negligible absorption at 2 μm (Type 4). These spectra could either be consistent with olivine or some

glasses, such as tektites or obsidian, which show little to no 2 μm band (**Figure 3**). Olivine displays a broad iron absorption band centered beyond 1 μm that can usually be distinguished from glass based on its strong shoulder near 1.25 μm, but the absorption band can become rounded to resemble glass upon substitution by other metals, mostly magnesium (King & Ridley, 1987). Glass spectra are sensitive to composition and cooling history (Minitti et al., 2002), and while glasses containing oxidized iron exhibit broad bands at both 1 and 2 μm, the 2 μm band is significantly diminished in glasses dominated by reduced iron (Cannon et al., 2017). In the sand sea surrounding the polar cap, spectra interpreted as glass exhibit weak or no 2 μm bands (Horgan & Bell, 2012). Thus, we hypothesize that spectra with a rounded (U-shaped) or narrow (V-shaped) symmetrical 1 μm absorption centered beyond 1.07 μm without a 1.3 μm shoulder are more consistent with glass, but may also be due to olivine or an olivine/glass mixture. Spectra with a relatively asymmetric 1 μm absorption that are often more V-shaped with a shoulder at 1.3 μm and centered at shorter wavelengths (~1.05 μm) are more consistent with olivine (s12 **Figure 4**).

Many spectra exhibit strong blue-slopes superposed over these mafic bands (s10–s12, s20 **Figure 4**) but sometimes the mafic bands can be entirely absent (s15 **Figure 2b**, s6 **Figure 3**). We interpret these dark and blue-sloped spectra as consistent with weathered (leached) glass, as previously detected in Siton Undae and other areas throughout the north polar sand sea (Figure 3; Horgan & Bell, 2012; Minitti et al., 2007). Within the NPLD, all of the mafic spectral signatures can be attributed to these endmembers or their mixtures.

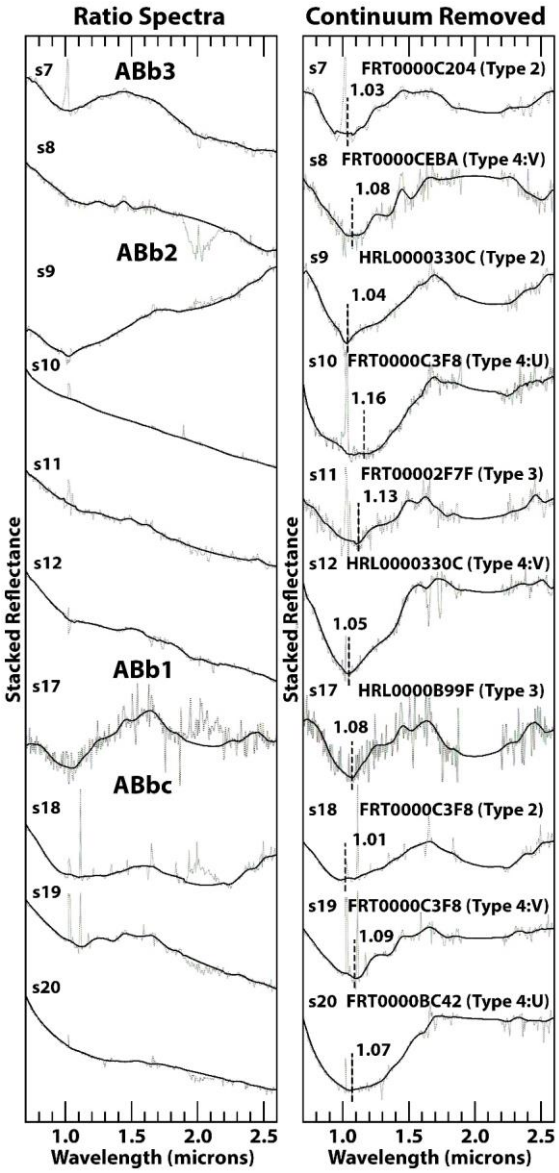

Figure 4: (*Left*) Ratio spectra and (*right*) continuum removed spectra of mafic materials detected within the lithic units of the NPLD. See **Figures 2**, **S2**, and **S3** for spectra locations.

3 Composition of Geologic Units within the NPLD

Geologic studies using satellite imagery have mapped various ice-rich lithic units within the NPLD (**Figure 1b** and **1c**) and have constrained their stratigraphic relationships and possible origins based on morphology (Tanaka et al., 2012). The uppermost unit, Planum Boreum 3 (ABb3), represents the ongoing deposition of volatiles in the current low obliquity period (Landis et al., 2016). Lithics within ABb3 include lag deposits in ablation zones and wind-blown

sediments eroding from underlying unit ABb1. Reflectance spectra of these areas are characterized as moderately dusty and dominated by water ice, however, ratio spectra either show weak mafic absorption bands (band depths less than 2%; s13 and s14 **Figure 2b;** s7 and s8 **Figure 4**) or steep blue-slope with no absorption band consistent with weathered glass (s15 **Figure 2b**). Absorption band centers for these spectra vary between 1.00 - 1.12 μm with little to no 2 μm absorption, indicating glass or olivine (Type 4: V) possibly mixed with some pyroxene (Type 2).

Planum Boreum 2 (ABb2) is a dark-toned sedimentary unit also known as the north polar "veneers", which may represent an unconformity within the NPLD. ABb2 is interpreted as either a distinct mantling deposit or an ablation lag, and the modern extent is likely due to wind transport toward the periphery of the polar cap (Rodriguez et al., 2007). Reflectance spectra from ABb2 are free of water ice absorptions and have low reflectance values indicating low dust cover. Upon ratioing, ABb2 spectra generally exhibit a strong blue sloped and concave-up shape, with a broad and symmetric 1 μm band centered at wavelengths longer than 1.07 μm and a shallow 2 μm band (s10 and s12 **Figure 4**; Type 4: U&V). These properties are consistent with a mixture dominated by weathered glass. Occasionally, spectra consistent with pyroxene (Type 2) and unweathered glass (Type 3) are detected within the ABb2 unit (s3 **Figure 3**; s9 and s11 **Figure 4**).

The unit forming most of the NPLD is the Planum Boreum 1 unit (ABb1) which is composed of thousands of meter-scale, horizontally stacked, and ice-rich layers, totaling up to 1500 m thick. Reflectance spectra from ABb1 contain the strongest dust signatures, possibly because each layer is a result of cyclic deposition and ablation processes, concentrating the seasonal dust as well as any deposited lithics, which makes them ideal targets for extracting climate records. While dust dominates (Type 1), ratio spectra with mafic absorption bands are also observed in ABb1 unit, primarily spectra without 2 μm bands that have V-shaped absorptions centered beyond 1.08 μm consistent with glass or olivine (Type 4; s5 **Figure 3**). Other spectra with 2 μm absorption bands exhibit glass-like absorptions (Type 3; s17 **Figure 4)**.

At lower elevations, the NPLD grades into the basal Cavi (ABbc) unit that is hypothesized to have formed during the Middle to Late Amazonian period (Tanaka et al., 2012). ABbc is marked by low albedo aeolian cross strata of water ice-cemented sandy material,

hypothesized to be an ancient polar dune field, which are inter-bedded with bright pure ice layers that may be remnants of ancient polar caps (Fishbaugh & Head, 2005; Tanaka et al., 2008). Spectrally, ABbc is less dusty and icy than overlying units, and therefore displays the strongest mafic signatures among all the NPLD units. However, the signatures vary significantly even within local outcrops. Strong HCP (Type 2) absorption bands (s2 **Figure 3** and s18 **Figure 4**) are observed, as well as both V- and U-shaped 1 μm absorptions beyond 1.075 μm (Type 4; s19 and s20 in **Figure 4**) with little to no 2 μm absorption band indicating the presence of glass or olivine (s15-s17 **Figure 4**). Finally, strongly blue-sloped spectra with no mafic bands consistent with weathered glass are also detected (s6 **Figure 3**).

The Rupes (ABbr) unit contains the oldest north polar sediments and forms most of the basal unit of the north polar deposits, which might have once been a 'paleo-plateau' (Tanaka et al., 2008). Early to Late Hesperian in age, Rupes is composed of layers of ice and fine-grained material over a kilometer thick, hypothesized to have been eroded and transported from the Scandia region (Tanaka et al., 2008, 2012). Surface spectra of Rupes appear dust and ice free, with a broad and symmetric absorption band at 1.1 μm and negligible absorption at 2 μm, most consistent with glass (Type 4; s4 **Figure 3**).

4 Volcanic and Impact Sediments within the NPLD

While glass and weathered glass signatures are the most widespread, mafic minerals like pyroxene, and likely olivine, are also common within the NPLD which suggests diverse sources and depositional processes. Mafic materials within the NPLD are broadly similar to those detected in the surrounding sand sea, but the mineralogy of lithics within the NPLD is spatially heterogenous, unlike the surrounding sand seas (Horgan & Bell, 2012). Diverse lithics eroding from NPLD troughs and scarps become well-mixed during aeolian transport into the sand seas, making it appear spectrally homogenous over vast expanse (Ewing et al., 2010; Tanaka et al., 2008). However, it is unlikely that the reverse case is true, that the NPLD lithics are aeolian sediments sourced from these dune fields or the surrounding plains. Wind models suggest that strong katabatic winds drive transport down off the cap and not up onto it (Smith & Spiga, 2018), so sediment is more likely to be emplaced onto the NPLD either ballistically or via atmospheric fallout. Compositional similarities to the surrounding plains may thus be due to both deposition of the same materials regionally and because the NPLD is a source of sediment for the

plains. The heterogeneity of the NPLD lithics also supports diverse origins unrelated to the sand sea. In particular, detection of olivine-like signatures within the NPLD suggests that at least some materials are sourced from far distances, since olivine signatures are only detected in bedrock or sediments on the surrounding plains at distances >1000 km (Salvatore et al., 2010).

We hypothesize that impact ejecta are a major source for mafic sediments in the NPLD. Impacts are frequent on Mars even today and are expected to ballistically deposit sediments locally and globally (Daubar et al., 2013). Proximal impact ejecta would contain a large fraction of diverse local country rock (e.g., pyroxene) and variable amounts of impact glass, with a grain-size decreasing with distance from the impact. Proximal ejecta could thus form locally thick impactite mantling layers over the NPLD, and we hypothesize that the ABb2 dark sedimentary mantle could be such an impactite deposit. Distal impacts would produce globally distributed mm to tens of cm thick layers of sand-sized glass (microtektites) or partially crystalline (microcrystites) spherules (Bouška & Bell, 1993). For example, a 15 km diameter crater can produce a global average of 40 microtektites per square centimeter (Lorenz, 2000). The iron in distal impact spherules is reduced during vaporization, causing a weaker 2 μm band consistent with Type 4 glassy spectra (**Figure 2b, 3** and **4**) observed within the NPLD. Larger tektites can be either glassy (Types 3 or 4) or crystalline (Type 2, pyroxene; Type 4, olivine) depending on their cooling history (Johnson & Melosh, 2014; Schultz & Mustard, 2004), therefore, distal ejecta could thus produce a mix of glassy and crystalline sand size mafic grains throughout the NPLD, consistent with the mafic sedimentary lags that we observe at the NPLD outcrops.

Mafic sediments at the NPLD could also be ash deposits sourced from volcanic eruptions. While the existence of volcanic edifices in the northern lowlands is controversial (Garvin et al., 2000), more distant sources could also have deposited ash, transported by atmospheric suspension and dispersed to distant locations by global atmospheric circulation (Kerber et al., 2012). Volcanic tephra can be crystalline or glass-rich, where glass abundances are significantly enhanced by water/ice interactions during eruption (Henderson et al., 2021; Wall et al., 2014). However, coarse (sand and larger) tephra is only deposited close to the source. Climate models suggest that only the finest-grained volcanic ash (particle size ~1 μm) can be latitudinally transported from the mid-latitudes and beyond to the poles, especially at low modern atmospheric densities (Kerber et al., 2012). Since no known major volcanoes are located at northern high-latitudes, any volcanic ash in the NPLD will account for a small volume of

sediment forming at least millimeter thick layers upon continued eruption over millions of years (Kerber et al., 2012). The most recent large volcanic eruptions on Mars are thought to have occurred only 1 to a few 10s of million years ago (Hartmann & Berman, 2000; Márquez et al., 2004; Neukum et al., 2004) so evidence of their eruption may exist within the NPLD.

In either case, NPLD would contain a unique record of the eruption and impact history of Mars during the late Amazonian, and sediments from these sources could provide both compositional markers for establishing stratigraphy across the region, as well as dateable minerals within the layers for quantitative geochronology using techniques like ^{40}Ar-^{39}Ar dating (Basile et al., 2001; Buizert et al., 2014). However, any landed mission analyzing the sediments for geochronology must consider the impact of local reworking of NPLD layers and sediments resulting from trough migration (Smith et al., 2013). Therefore, landing sites for these missions must target least impacted stratigraphic horizons. Extracting ice cores and constraining dates for climate records will provide better constraints on the effects of astronomical forcing (Levrard et al., 2007) and stochastic processes like impacts (Perron & Huybers, 2009) on planetary climatology, as well as substantially improve our understanding of modern sediment sources on Mars, the evolution of the martian interior, and the recent impact flux at Mars (Banfield et al., 2020).

5 Significance of dust and non-dust lithics in the NPLD

The NPLD are typically modeled as a simple mixture of ice and martian airfall dust (containing nanophase ferric oxides with other amorphous and crystalline minerals; Ehlmann et al., 2017), varying from ~95% ice to up to ~50% dust, based on radar models and spectral observations (Calvin et al., 2009; Lalich et al., 2019). However, this simple model is inconsistent with detections of coarse-grained mafic sediment, which suggests that lithics are entrained within the NPLD through a combination of dust falling on the surface, deposits of lithic sediments sourced from impacts and volcanic eruptions, and ablation, leading to stratigraphic variations in the concentration of both types of lithics.

Airfall martian dust is the largest and most continuous source of refractory lithic material to the NPLD. Atmospheric dust changes energy flux in the atmosphere which has the potential to be a major internal driver of climate variations on Mars (Kahre et al., 2017). These climatic variations can alter the atmospheric state and thereby its ability to access different reservoirs of

dust across the planet. Hence, the concentration and composition of dust in the NPLD may provide records of major dust events or cycles, and may reflect temporal variations in dust composition and characteristics sourced from different regions of Mars under changing climatic conditions.

Although the NPLD contains mafic materials, the nature of their occurrence varies. The RGB spectral parameter color-composite images in **Figure 2** show that the NPLD (unit ABb1 in red) forming upper Planum Boreum is comprised of a stack of icy layers and thin ablation lags that are ferric-dust rich with minor and spatially variable components of both crystalline and glass-rich mafic sediments that we interpret as sourced from impacts and volcanism. The underlying Cavi unit (ABbc in blue/green) is sand-rich and dominated by locally heterogeneous mafic sediments. The heterogeneity suggests that the Cavi is not just well-mixed sands similar to and perhaps sourced from the surrounding dune fields, and that it may contain materials from ballistic sources as well. The polar veneers (ABb2 in green) that mantle the NPLD are dominated by much more homogeneous glass-rich materials. The homogeneity suggests that this unit could either represent a deposit from a distinct mantling event or an ablation lag reworked by aeolian processes to concentrate sand-sized glassy materials.

Concentration of coarse glassy sediments during ablation of the NPLD appears to be actively occurring today in the north polar troughs (**Figure 2b**). Solar insolation and katabatic winds erode the equatorward-facing slope (magenta in **Figure 2b**), blowing away fine-grained ferric-dust and lithic fragments and concentrating reworked coarse glass-rich sediments (green/blue in **Figure 2b**) at the trough bottom and over the poleward facing slope. This observation strongly supports an ablation lag origin for the similarly glass-rich and sand-size sediments of the veneers/ABb2 unit, which we hypothesize contains significant abundances of coarse glassy grains originating as distal impact spherules, possibly from a large number of impact events. Determining the range of ages of sediments in this unit could thus provide both an important stratigraphic marker within the NPLD and a critical constraint on the impact flux at Mars during the Amazonian.

Past mantling by impact ejecta, ash, a dust event, or an ablation lag has major implications for the thermal stability, strength of the stratified structure, and the age of ice at the NPLD (Levrard et al., 2007; Smith, 2020; Sori et al., 2016). The presence of lithics other than

dust may increase the thickness and insulating properties of sublimation lag deposits, which controls ablation rates of underlying ice, and hence, the time taken to build or remove the layers forming the NPLD. For example, the ABb2 dark sedimentary unit could represent a major lag that once covered the NPLD, which may have increased the stability of the NPLD during the most recent periods of high obliquity.

Lithics in the NPLD also record the recent history of water activity at the north pole. Detection of weathered glass, which if altered in situ, suggests water activity in the recent past of the NPLD. At the low temperatures of the NPLD, liquid water brines can persist as thin film surrounding lithic sediments which causes acid leaching of cations and forming weathering rinds on the surface of glassy sediments (Chemtob et al., 2010; Minitti et al., 2007). The NPLD and surrounding regions are known to contain sulfates (Horgan et al., 2009; Massé et al., 2010, 2012) and other salts (Toner et al., 2014), that may have formed by alteration of lithics surrounded by ice-brine slush or episodic interactions with groundwater. The degree of aqueous activity is perhaps controlled by climate change caused by astronomical forcing or due to discrete stochastic events related to impacts or volcanic eruptions, which would have directly influenced the habitability of Mars' polar terrains.

6 Conclusions

Our analysis shows a significant concentration of lithics other than airfall ferric-dust throughout the NPLD, and detections include both glass and crystalline mafic minerals. Glasses are a dominant material throughout the NPLD suggesting that impact ejecta such as distal impact spherules has been a major source of sand-sized sediment. Volcanic ash is likely to be present but primarily as very fine-grained sediments. Thus, this study demonstrates that along with martian dust cycles, geologic processes like impacts and volcanic eruptions during the late Amazonian influenced formation of the NPLD by depositing material from regional and global sources. The role of these stochastic geological processes and subsequent reworking over the polar cap, due to ablation and aeolian activity, must be factored into radar and climate models to improve estimates of the NPLD's physical properties and timing of accumulation. The presence of dateable sediments within the NPLD make it an excellent site for assessing recent rates of impacts and volcanic activity, and carrying out a first paleoclimate study using landed robotic

asset on another planet that is devoid of climate complicating factors such as oceans, biology, etc. (Smith et al., 2020).

Acknowledgments

This research was funded by Future Investigators in NASA Earth and Space Science and Technology (FINESST) award number 80NSSC19K1535.

Open Research

CRISM images are available on NASA's Planetary Data System (PDS) Geoscience Node archive (https://pds-geosciences.wustl.edu/missions/mro/crism.htm). All spectral data and processing details are included in the supporting documents.

References

Banfield, D., Stern, J., Davila, A., Johnson, S. S., Brain, D., Wordsworth, R., et al. (2020). Mars Science Goals, Objectives, Investigations, and Priorities: 2020 Version. *Mars Exploration Program Analysis Group (MEPAG)*.

Basile, I., Petit, J. R., Touron, S., Grousset, F. E., & Barkov, N. (2001). Volcanic layers in Antarctic (Vostok) ice cores: Source identification and atmospheric implications. *Journal of Geophysical Research: Atmospheres*, *106*(D23), 31915–31931.

Becerra, P., Sori, M. M., & Byrne, S. (2017). Signals of astronomical climate forcing in the exposure topography of the North Polar Layered Deposits of Mars. *Geophysical Research Letters*, *44*(1), 62–70.

Bouška, V., & Bell III, J. F. (1993). Assumptions about the presence of natural glasses on Mars. *Journal of Geophysical Research: Planets*, *98*(E10), 18719–18725.

Buizert, C., Baggenstos, D., Jiang, W., Purtschert, R., Petrenko, V. v, Lu, Z.-T., et al. (2014). Radiometric 81Kr dating identifies 120,000-year-old ice at Taylor Glacier, Antarctica. *Proceedings of the National Academy of Sciences*, *111*(19), 6876–6881.

Calvin, W. M., Roach, L. H., Seelos, F. P., Seelos, K. D., Green, R. O., Murchie, S. L., & Mustard, J. F. (2009). Compact Reconnaissance Imaging Spectrometer for Mars observations of northern Martian latitudes in summer. *Journal of Geophysical Research: Planets*, *114*(E2).

Cannon, K. M., Mustard, J. F., Parman, S. W., Sklute, E. C., Dyar, M. D., & Cooper, R. F. (2017). Spectral properties of Martian and other planetary glasses and their detection in remotely sensed data. *Journal of Geophysical Research: Planets*, *122*(1), 249–268.

Chemtob, S. M., Jolliff, B. L., Rossman, G. R., Eiler, J. M., & Arvidson, R. E. (2010). Silica coatings in the Ka'u Desert, Hawaii, a Mars analog terrain: A micromorphological, spectral, chemical, and isotopic study. *Journal of Geophysical Research: Planets*, *115*(E4).

Cloutis, E. A., & Gaffey, M. J. (1991). Pyroxene spectroscopy revisited: Spectral-compositional correlations and relationship to geothermometry. *Journal of Geophysical Research: Planets*, *96*(E5), 22809–22826.

Cutts, J. A. (1973). Nature and origin of layered deposits of the Martian polar regions. *Journal of Geophysical Research*, *78*(20), 4231–4249.

Daubar, I. J., McEwen, A. S., Byrne, S., Kennedy, M. R., & Ivanov, B. (2013). The current martian cratering rate. *Icarus*, *225*(1), 506–516.

Ehlmann, B. L., Edgett, K. S., Sutter, B., Achilles, C. N., Litvak, M. L., Lapotre, M. G. A., et al. (2017). Chemistry, mineralogy, and grain properties at Namib and High dunes, Bagnold dune field, Gale crater, Mars: A synthesis of Curiosity rover observations. *Journal of Geophysical Research: Planets*, *122*(12), 2510–2543.

Ewing, R. C., Peyret, A. B., Kocurek, G., & Bourke, M. (2010). Dune field pattern formation and recent transporting winds in the Olympia Undae Dune Field, north polar region of Mars. *Journal of Geophysical Research: Planets*, *115*(E8).

Fishbaugh, K. E., & Head III, J. W. (2005). Origin and characteristics of the Mars north polar basal unit and implications for polar geologic history. *Icarus*, *174*(2), 444–474.

Fishbaugh, K. E., Byrne, S., Herkenhoff, K. E., Kirk, R. L., Fortezzo, C., Russell, P. S., & McEwen, A. (2010). Evaluating the meaning of "layer" in the Martian north polar layered deposits and the impact on the climate connection. *Icarus*, *205*(1), 269–282.

Garvin, J. B., Sakimoto, S. E. H., Frawley, J. J., Schnetzler, C. C., & Wright, H. M. (2000). Topographic evidence for geologically recent near-polar volcanism on Mars. *Icarus*, *145*(2), 648–652.

Hartmann, W. K., & Berman, D. C. (2000). Elysium Planitia lava flows: Crater count chronology and geological implications. *Journal of Geophysical Research: Planets*, *105*(E6), 15011–15025.

Henderson, M. J. B., Horgan, B. H. N., Rowe, M. C., Wall, K. T., & Scudder, N. A. (2021). Determining the Volcanic Eruption Style of Tephra Deposits From Infrared Spectroscopy. *Earth and Space Science*, *8*(2), e2019EA001013.

Horgan, B., & Bell III, J. F. (2012). Widespread weathered glass on the surface of Mars. *Geology*, *40*(5), 391–394.

Horgan, B. H., Bell III, J. F., Noe Dobrea, E. Z., Cloutis, E. A., Bailey, D. T., Craig, M. A., et al. (2009). Distribution of hydrated minerals in the north polar region of Mars. *Journal of Geophysical Research: Planets*, *114*(E1).

Horgan, B. H. N., Cloutis, E. A., Mann, P., & Bell III, J. F. (2014). Near-infrared spectra of ferrous mineral mixtures and methods for their identification in planetary surface spectra. *Icarus*, *234*, 132–154.

Johnson, B. C., & Melosh, H. J. (2014). Formation of melt droplets, melt fragments, and accretionary impact lapilli during a hypervelocity impact. *Icarus*, *228*, 347–363.

Kahre, M. A., Murphy, J. R., Newman, C. E., Wilson, R. J., Cantor, B. A., Lemmon, M. T., & Wolff, M. J. (2017). The Mars dust cycle. *The Atmosphere and Climate of Mars*, *18*, 295.

Kerber, L., Head, J. W., Madeleine, J.-B., Forget, F., & Wilson, L. (2012). The dispersal of pyroclasts from ancient explosive volcanoes on Mars: Implications for the friable layered deposits. *Icarus*, *219*(1), 358–381.

King, T. V. v, & Ridley, W. I. (1987). Relation of the spectroscopic reflectance of olivine to mineral chemistry and some remote sensing implications. *Journal of Geophysical Research: Solid Earth*, *92*(B11), 11457–11469.

Lalich, D. E., Holt, J. W., & Smith, I. B. (2019). Radar reflectivity as a proxy for the dust content of individual layers in the Martian north polar layered deposits. *Journal of Geophysical Research: Planets*, *124*(7), 1690–1703.

Landis, M. E., Byrne, S., Daubar, I. J., Herkenhoff, K. E., & Dundas, C. M. (2016). A revised surface age for the North Polar Layered Deposits of Mars. *Geophysical Research Letters*, *43*(7), 3060–3068.

Levrard, B., Forget, F., Montmessin, F., & Laskar, J. (2007). Recent formation and evolution of northern Martian polar layered deposits as inferred from a Global Climate Model. *Journal of Geophysical Research: Planets*, *112*(E6).

Márquez, Á., Fernández, C., Anguita, F., Farelo, A., Anguita, J., & de la Casa, M.-A. (2004). New evidence for a volcanically, tectonically, and climatically active Mars. *Icarus*, *172*(2), 573–581.

Massé, M., Bourgeois, O., le Mouélic, S., Verpoorter, C., le Deit, L., & Bibring, J.-P. (2010). Martian polar and circum-polar sulfate-bearing deposits: Sublimation tills derived from the North Polar Cap. *Icarus*, *209*(2), 434–451.

Massé, M., Bourgeois, O., le Mouélic, S., Verpoorter, C., Spiga, A., & le Deit, L. (2012). Wide distribution and glacial origin of polar gypsum on Mars. *Earth and Planetary Science Letters*, *317*, 44–55.

Minitti, M. E., Mustard, J. F., & Rutherford, M. J. (2002). Effects of glass content and oxidation on the spectra of SNC-like basalts: Applications to Mars remote sensing. *Journal of Geophysical Research: Planets*, *107*(E5), 1–6.

Minitti, M. E., Weitz, C. M., Lane, M. D., & Bishop, J. L. (2007). Morphology, chemistry, and spectral properties of Hawaiian rock coatings and implications for Mars. *Journal of Geophysical Research: Planets*, *112*(E5).

Morris, R. v, & Lauer Jr, H. v. (1990). Matrix effects for reflectivity spectra of dispersed nanophase (superparamagnetic) hematite with application to Martian spectral data. *Journal of Geophysical Research: Solid Earth*, *95*(B4), 5101–5109.

Morris, R. v, Golden, D. C., & Bell III, J. F. (1997). Low-temperature reflectivity spectra of red hematite and the color of Mars. *Journal of Geophysical Research: Planets*, *102*(E4), 9125–9133.

Neukum, G., Jaumann, R., Hoffmann, H., Hauber, E., Head, J. W., Basilevsky, A. T., et al. (2004). Recent and episodic volcanic and glacial activity on Mars revealed by the High Resolution Stereo Camera. *Nature*, *432*(7020), 971–979.

Perron, J. T., & Huybers, P. (2009). Is there an orbital signal in the polar layered deposits on Mars? *Geology*, *37*(2), 155–158.

Rodriguez, J. A. P., Tanaka, K. L., Langevin, Y., Bourke, M., Kargel, J., Christensen, P., & Sasaki, S. (2007). Recent aeolian erosion and deposition in the north polar plateau of Mars. *Mars Journal*, *3*.

Salvatore, M. R., Mustard, J. F., Wyatt, M. B., & Murchie, S. L. (2010). Definitive evidence of Hesperian basalt in Acidalia and Chryse planitiae. *Journal of Geophysical Research: Planets*, *115*(E7).

Schultz, P. H., & Lutz, A. B. (1988). Polar wandering of Mars. *Icarus*, *73*(1), 91–141.

Schultz, P. H., & Mustard, J. F. (2004). Impact melts and glasses on Mars. *Journal of Geophysical Research: Planets*, *109*(E1).

Smith, I B. (2020). A Hypothesis for the" No-Flow" Mars' North Polar Layered Deposits Observations. *LPI Contributions*, *2099*, 6040.

Smith, Isaac B, & Spiga, A. (2018). Seasonal variability in winds in the north polar region of Mars. *Icarus*, *308*, 188–196.

Smith, Isaac B, Holt, J. W., Spiga, A., Howard, A. D., & Parker, G. (2013). The spiral troughs of Mars as cyclic steps. *Journal of Geophysical Research: Planets*, *118*(9), 1835–1857.

Smith, Isaac B, Putzig, N. E., Holt, J. W., & Phillips, R. J. (2016). An ice age recorded in the polar deposits of Mars. *Science*, *352*(6289), 1075–1078.

Smith, Isaac B, Hayne, P. O., Byrne, S., Becerra, P., Kahre, M., Calvin, W., et al. (2020). The Holy Grail: A road map for unlocking the climate record stored within Mars' polar layered deposits. *Planetary and Space Science*, *184*, 104841.

Soare, R. J., Horgan, B., Conway, S. J., Souness, C., & El-Maarry, M. R. (2015). Volcanic terrain and the possible periglacial formation of "excess ice" at the mid-latitudes of Utopia Planitia, Mars. *Earth and Planetary Science Letters*, *423*, 182–192.

Sori, M. M., Byrne, S., Hamilton, C. W., & Landis, M. E. (2016). Viscous flow rates of icy topography on the north polar layered deposits of Mars. *Geophysical Research Letters*, *43*(2), 541–549.

Tanaka, K. L., Rodriguez, J. A. P., Skinner Jr, J. A., Bourke, M. C., Fortezzo, C. M., Herkenhoff, K. E., et al. (2008). North polar region of Mars: Advances in stratigraphy, structure, and erosional modification. *Icarus*, *196*(2), 318–358.

Tanaka, K. L., Fortezzo, C. M., & Ryan, D. A. (2012). *Geologic map of the north polar region of Mars*. US Department of the Interior, US Geological Survey.

Toner, J. D., Catling, D. C., & Light, B. (2014). Soluble salts at the Phoenix Lander site, Mars: A reanalysis of the Wet Chemistry Laboratory data. *Geochimica et Cosmochimica Acta*, *136*, 142–168.

Toon, O. B., Pollack, J. B., Ward, W., Burns, J. A., & Bilski, K. (1980). The astronomical theory of climatic change on Mars. *Icarus*, *44*(3), 552–607.

Viviano-Beck, C. E., Seelos, F. P., Murchie, S. L., Kahn, E. G., Seelos, K. D., Taylor, H. W., et al. (2014). Revised CRISM spectral parameters and summary products based on the currently detected mineral diversity on Mars. *Journal of Geophysical Research: Planets*, *119*(6), 1403–1431.

Wall, K. T., Rowe, M. C., Ellis, B. S., Schmidt, M. E., & Eccles, J. D. (2014). Determining volcanic eruption styles on Earth and Mars from crystallinity measurements. *Nature Communications*, *5*(1), 1–8.

Reference (Supporting Information)

Bennett, K. A., Horgan, B. H. N., Gaddis, L. R., Greenhagen, B. T., Allen, C. C., Hayne, P. O., et al. (2016). Complex explosive volcanic activity on the Moon within Oppenheimer crater. *Icarus*, *273*, 296–314.

Bibring, J.-P., Langevin, Y., Gendrin, A., Gondet, B., Poulet, F., Berthé, M., et al. (2005). Mars surface diversity as revealed by the OMEGA/Mars Express observations. *Science*, *307*(5715), 1576–1581.

Cloutis, E. A., & Gaffey, M. J. (1991). Pyroxene spectroscopy revisited: Spectral-compositional correlations and relationship to geothermometry. *Journal of Geophysical Research: Planets*, *96*(E5), 22809–22826.

Horgan, B., & Bell III, J. F. (2012). Widespread weathered glass on the surface of Mars. *Geology*, *40*(5), 391–394.

Horgan, B. H. N., Cloutis, E. A., Mann, P., & Bell III, J. F. (2014). Near-infrared spectra of ferrous mineral mixtures and methods for their identification in planetary surface spectra. *Icarus*, *234*, 132–154.

King, T. V. v, & Ridley, W. I. (1987). Relation of the spectroscopic reflectance of olivine to mineral chemistry and some remote sensing implications. *Journal of Geophysical Research: Solid Earth*, *92*(B11), 11457–11469.

McGuire, P. C., Wolff, M. J., Smith, M. D., Arvidson, R. E., Murchie, S. L., Clancy, R. T., et al. (2008). MRO/CRISM retrieval of surface Lambert Albedos for multispectral mapping of Mars with DISORT-based radiative transfer modeling: Phase 1—Using historical climatology for temperatures, aerosol optical depths, and atmospheric pressures. *IEEE Transactions on Geoscience and Remote Sensing*, *46*(12), 4020–4040.

Minitti, M. E., Mustard, J. F., & Rutherford, M. J. (2002). Effects of glass content and oxidation on the spectra of SNC-like basalts: Applications to Mars remote sensing. *Journal of Geophysical Research: Planets*, *107*(E5), 1–6.

Murchie, S., Arvidson, R., Bedini, P., Beisser, K., Bibring, J., Bishop, J., et al. (2007). Compact reconnaissance imaging spectrometer for Mars (CRISM) on Mars reconnaissance orbiter (MRO). *Journal of Geophysical Research: Planets*, *112*(E5).

Murchie, S. L., Seelos, F. P., Hash, C. D., Humm, D. C., Malaret, E., McGovern, J. A., et al. (2009). Compact Reconnaissance Imaging Spectrometer for Mars investigation and data set from the Mars Reconnaissance Orbiter's primary science phase. *Journal of Geophysical Research: Planets*, *114*(E2).

Seelos, F. P., Murchie, S. L., Humm, D. C., Barnouin, O. S., Morgan, F., Taylor, H. W., et al. (2011). CRISM data processing and analysis products update—Calibration, correction, and visualization. In *Lunar and Planetary Science Conference* (p. 1438).

Sinha, P., Horgan, B., & Seelos, F. (2019). Dateable Volcanic and Impact Sediments within the North Polar Layered Deposits on Mars. In *Lunar and Planetary Science Conference* (p. 2027).

Viviano-Beck, C. E., Seelos, F. P., Murchie, S. L., Kahn, E. G., Seelos, K. D., Taylor, H. W., et al. (2014). Revised CRISM spectral parameters and summary products based on the currently detected mineral diversity on Mars. *Journal of Geophysical Research: Planets*, *119*(6), 1403–1431.

Wiseman, S. M., Arvidson, R. E., Morgan, F., Wolff, M. J., Morris, R. v, McGuire, P. C., et al. (2010). Radiative Transfer Modeling of the Empirical'Volcano Scan'Atmospheric Correction: Discussion of Artifacts. In *Lunar and Planetary Science Conference* (p. 2461).